

**STRUCTURAL AND ANTIMICROBIAL PROPERTIES OF 3-[2-(1,5-DIMETHY 3-
OXO-2-PHENYL-2,3-DIHYDRO-1H-PYRAZOL-4-YL) HYDRAZILIDINE]-1,3-
DIPHENYLPROPANE-1,3-DIONE AND ITS Co(II), Fe(III), Cu(II) AND Ni(II)
COMPLEXES**

N.J. Agbo^{1*} and P.O. Ukoha²

¹Chemistry Advanced Research Centre, Sheda and Science and Technology Complex
(SHESTCO), Garki-Abuja, Nigeria

²Coordination Chemistry and Inorganic Pharmaceutical Unit Department of Pure and Industrial
Chemistry, University of Nigeria, Nsukka, Enugu State, Nigeria 41001

(Received March 8, 2024; Revised September 2, 2024; Accepted September 2, 2024)

ABSTRACT. This work aims at synthesizing new hydrazone molecules with enhanced antibacterial capabilities. Diazotized 4-aminoantipyrine and 1,3-diphenyl-1,3-dione were coupled at around 5 °C to yield 3-[2-(1,5-dimethyl-3-oxo-2-phenyl-2,3-dihydro-1H-pyrazol-4-yl) hydrazilidene]1,3-dione-1,3-diphenylpropane (HPDP). Its Co(II), Fe(III), Cu(II), and Ni(II) complexes were formed by refluxing stoichiometric amounts of chloride salts in separately with HPDP for 6 hours at 60 °C. HPDP and its complexes were characterized by means of spectroscopic techniques, conductivity, micro elemental analysis and melting point. Only HPDP X-ray diffraction spectral was obtained. The *in-vitro* antibacterial tests of compounds were done on *Bacillus subtilis*, *Streptococcus pneumoniae*, *Pseudomonas aeruginosa*, *Escherichia coli* (*Eco 6* and *Eco 13*), *Staphylococcus aureus*, *Protus*, *Staphylococcus intermedius* (*G101*), *Klebsiella pneumoniae* and *Salmonella Typhi*. Spectroscopic studies show that HPDP is terdentately coordinated to the metal ion to form octahedral complexes with the acetyl, hydrazinyl nitrogen, and pyrazolone ring carbonyl groups. HPDP crystallized as monochronic with space group *PbCa* and unit dimensions $a = 9.5528(8)$ Å, $\alpha = 90^\circ$; $b = 19.6260(16)$ Å, $\beta = 101.426(6)^\circ$; $c = 12.058(10)$ Å, $\gamma = 90^\circ$ for $z = 4$. Antimicrobial evaluations show that HPDP and [Ni(PDP)₂] exhibited antibacterial activity against *Salmonella Typhi* and *Staphylococcus aureus* up to the least concentration (0.31 µg/cm³), suggesting their potential for application as antibacterial drugs.

KEY WORDS: Selenium, Amino acids, Vitamin B3, Mixed ligand, Complexes, Antioxidant

INTRODUCTION

Hydrazines can combine with ketones or aldehydes to generate hydrazones [1, 2], or aryl diazonium salts can react with β-ketoacids and β-ketoesters [3]. The versatility of hydrazones as antibacterial, analgesic, anti-inflammatory, antiplatelet, antituberculosis, and anticancer drugs has led to a spike in interest in their investigation [4-6]. Other hydrozotics like those generated from 2,3,4-pentanetrione, N1-(4-methoxybenzamido benzoyl, and 4-hydroxybenzoic acid [(5-nitro-2-furyl) methylene] hydrazide (niferoxazide) is an intestinal antiseptic, and isotinyl hydrazones have been shown to have antitubercular properties [7].

Transition metal ions can form stable complexes with hydrozone, an extremely flexible ligand. These ligands have been used as model compounds in analytical and bioinorganic chemistry [8]. It has been found that coordination compounds generated from aroylhydrazones exhibit good pharmacological applicability and function as enzyme inhibitors [9, 10].

There is little information available about this particular hydrazone, which was derived from the combination of 1,3-diphenylpropane-1,3-dione and 4-aminoantipyrine. The use of this particular compound as antimicrobial medications has not been reported. It will be quite interesting to produce antimicrobial medications from these two compounds by utilizing the pharmacological activities of 4-aminoantipyrine and the proven activities of hydrazones [13]. As a result, we synthesized the hydrazone HPDP by combining 1,3-diphenylpropane-1,3-dione with

*Corresponding authors. E-mail: agbo.ndj@gmail.com

This work is licensed under the Creative Commons Attribution 4.0 International License

its Co(II), Cu(II), Ni(II), and Fe(III) complexes with diazotized 4-aminoantipyrene. It is well known that complex formation improves ligands' physiological characteristics [14]. The antibacterial potentials of the ligand and complexes were identified.

EXPERIMENTAL

All chemicals used (4-amino antipyrene, 1,3-diphenylpropane-1,3-dione, sodium acetate, sodium nitrite, ethanol, methanol) were analytical grade and were products of Sigma Aldrich. They were used as purchased without further purification unless otherwise stated.

Heating was done on Gallonkamp Magnetic Stirrer/Thermostat hot plate. John-Fisher melting point apparatus was used in determining melting points of compounds. UV Visible spectra were obtained on Cecil-UV-Visible spectrophotometer whereas Perkin-Elmer FTIR spectrometer and Bruker DPX 400 NMR spectrophotometer used to run ^1H and ^{13}C spectra of compounds. Single crystal X-ray diffraction data of HPDP was obtained on a Goniometer of Kappa geometry and CCD diffraction equipped with Mo, $K\alpha$ source crystallographic data were corrected for absorption and polarization effects. Carbon, hydrogen and nitrogen were determined on a Heraeus Carlo Erba 1108-CHN Analyser. Conductivity of 1.0×10^{-3} mol dm^{-3} methanolic solution of compounds were determined using WTW-LF90 conductivity.

Synthesis of the ligand (HPDP)

Heinosuke's method [15] was employed for synthesizing HPDP. 4-Aminoantipyrene (0.1884 g, 0.0006 mol) was dissolved in dil. HCl and diazotized with 0.06 g/10 cm^3 aqueous solution of NaNO_2 5 °C. The diazonium salt was reacted with 6.0×10^{-4} mol dm^{-3} . 1,3-Diphenylpropane-1,3-dione in sodium acetate (2.5 g in 150 cm^3 H_2O). The precipitate formed was filtered, washed with methanol/water, recrystallized and stored over CaCl_2 in a desiccator.

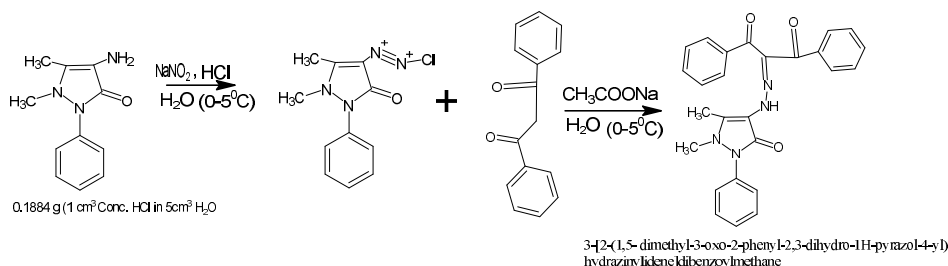
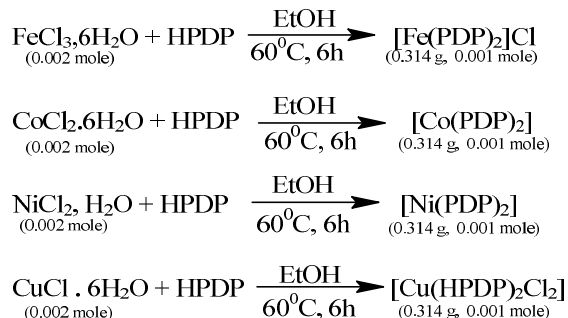


Figure 1. Synthesis of the ligand.

Synthesis of complexes

Chloride salts of Fe(III), Cu(II), Co(II) and Ni(II) were reacted separately with HPDP in a 2:1 mole ratio in 50 cm^3 ethanol following the method of El. Saied *et.al* [16]. The mixtures were refluxed for 6 h at 60 °C. The precipitates formed were filtered, dried and stored over CaCl_2 in a desiccator.

Metal Salts:



Scheme 1. Equation reaction.

Antibacterial screening

The microorganisms used: *Pseudomonas aeruginosa*, *Bacillus subtilis*, *Staphylococcus aureus*, *Escherichia coli* (*Eco* 6 and *Eco*.13), *Streptococcus pneumoniae*, and *Staphylococcus intermedius* (*G101*) were clinical isolates from human, while *Protus mirabilis*, and *Klebsiella pneumoniae* were clinical isolates from Pig from faculty of veterinary Medicine, University of Nigeria Nsukka. Established method [17, 18] were adopted to determine the sensitivity of the different bacterial strains to DMO solutions of the ligand and complexes. Agar-well diffusion method using Nutrient Agar and Sabouraud Dextrose Agar (SDA) inoculated with 0.1 cm³ broth culture of test bacteria was performed.

HPDP and the complexes (50 mg in DMSO) at concentrations of 0.156 to 10 mg/mL were used by filling the bored wells of the agar with 0.5 cm³ of the compounds. Ciprofloxacin, Ampicillin and Gentamycin were used as positive control while sterile DMO was used as negative control. The plates were incubated at 37 °C for 24 h after which inhibition zone diameters (IZD) were measured. Antilog of intercept on y-axis of plots of IZD² versus log (concentration) gave the minimum inhibitory concentration (MIC).

RESULTS AND DISCUSSION*Physical properties of HPDP and its complexes*

Yield and some of the physical properties of HPDP and its Co(II), Fe(III), Ni(II) and Cu(II) complexes are presented in Table 1. The different colors, yield and melting points of the complexes are high indicators to formation of new compounds from the reaction of the ligand with the metal salts. Comparing the conductivity of the ligand and complexes with KCl (1:1 electrolyte) and CuSO₄ (2:2 electrolytes), it is very obvious that Fe(III) complex with conductivity close to CuSO₄ is an electrolyte (cationic complex) whereas the ligand and other complexes are neutral and non-electrolytes. The formulae they are given also suggest this.

C, H, N microanalysis and mass spectral data

Carbon, hydrogen and nitrogen content of the ligand and complexes are given in Table 2. The percentage of the elements present determined experimentally is compared with theoretical predictions. These were very close agreement with the values thereby confirming synthesis of the compounds.

Table 1. Physical properties of HPDP and its complexes.

Compound	Colour	Texture	%Yield	Melting point/ ^o C	Conductivity/ (S/cm)	Cl ⁻
HPDP	Orange	Powder	29.05 ± 0.58	73 - 74	2.10x10 ⁻⁷	-
[Fe(PDP) ₂]Cl	Brown	Granular	65.00 ± 1.30	162.16	1.90x10 ⁻⁴	Present (O.S.)
[Co(PDP) ₂]	Black	Granular	51.34 ± 1.02	69.70	3.7x10 ⁻⁷	Absent
[Cu(HPDP) ₂ Cl ₂]	Black	Granular	67.34 ± 1.34	43.44	6.7x10 ⁻⁷	Present (I.S.)
[Ni(PDP) ₂]	Brown	Granular	54.47 ± 1.09	65.64	3.0x10 ⁻⁷	Absent
KCl	-	-	-	-	1.76x10 ⁻³	-
CuSO ₄	-	-	-	-	7.6x10 ⁻⁴	-

Legend: O.S. = outer-sphere; I.S. = inner-sphere, mean ± standard deviation (SD) with n = 2 for % yield.

Table 2. Elemental analysis of the HPDP and its complexes.

Element	Values	HPDP	[Fe(PDP) ₂]Cl	[Co(PDP) ₂]	[Cu(HPDP) ₂ Cl ₂]	[Ni(PDP) ₂]
C	Found %	69.86	64.02	66.22	59.73	74.68
	Cal. %	71.20	64.63	66.87	61.15	74.56
H	Found %	4.70	4.99	4.90	4.9	4.77
	Cal. %	5.06	4.38	4.533	4.39	5.06
N	Found %	11.57	11.38	11.57	11.425	11.54
	Cal. %	12.77	11.59	11.99	11.08	13.08

The mass spectrum of HPDP shows a base peak of 464.5385 to which is also the molecular ion peak. The m/z values of 464.5385 represents the molecular weight of HPDP (C₂₆H₂₂N₄O₃) of 438.46 plus two Na⁺ attached (m+2Na⁺) as scavenging ion. Fragment at m/z of 384.336 is most likely for [C₂₀H₁₇N₄O₃]⁺ where one phenyl group has been removed. Also, m/z of 306.480 is probably due to removal of the second phenyl group to give (C₁₄H₁₂N₄O₃)⁺.

Electronic spectral data of HPDP and the complexes

Table 3 shows the wave length of maximum absorption as the molar absorptivities of ligand and complexes. The solution spectra were obtained in methanol. HPDP has two peaks at 368 and 448 nm which are attributable n→π* to transition intraligand. The molar absorptivities which are within 176 to 178 dm³mol⁻¹cm⁻¹ are agreement with n→π* transition [19]. The strong K band expected for azo compounds at 270-280 nm is absent thereby indicating non-formation of azo compound but likely a hydrazone [20].

Table 3. Electronic spectra of HPDP and its complexes.

Compounds	λ _{max} (nm)	λ (cm ⁻¹)	ε (dm ³ mol ⁻¹ cm ⁻¹)	Assignment
HPDP	368	27174	178.158	n→π*
	448	22321	176.140	n→π*
[Fe(PDP) ₂]Cl	375	26667	51.8672	π→π*
	479	20877	28.0082	n→π*
	564.3	17721	20.7468	Charge Transfer
	650	15385	20.7468	Charge Transfer
[Co(PDP) ₂]	742	13477	10.3734	Charge Transfer
	592.9	16867	40.4563	⁴ t _{1g} (f) → ⁴ a _{2g} (f)
	746.4	13397	49.0353	d←d
[Cu(HPDP) ₂ Cl ₂]	428	23364	371.059	d←d
[Ni(PDP) ₂]	283	35335	919.11	π→π*
	360	27778	264.361	n→π*

[Fe(HPDP)₂]Cl has absorption peaks at 375, 479, 565, 650 and 742 nm. These weak bands (ϵ_{\max} between 10 and 51 dm³ mol⁻¹cm⁻¹) are most likely due to forbidden transition in a high spin d⁵ octahedral complex. since all transitions from t_{2g} to e_g levels will be spin forbidden, no exacted of the same spin multiplicity with the ground state will arise. Hence, only weak bands arising from vibrational motions that acts continually to slightly distort the molecular symmetry [21, 22]. The bands at 375 nm, 479 nm will slightly enhanced ϵ_{\max} as mostly like combination transition involving both forbidden d←d and ligand to metal or metal to ligand charge transfer. These band confirm [Fe(PDP)₂]Cl to be octahedral and high spin. Complication in the spectral are typical of operation of intraligand transition with metal based transition in complexes.

The Co(II) complex, [Co(PDP)₂], shows two prominent bands at 592.9 and 746 nm with absorption between 40 and 49 dm³ mol⁻¹cm⁻¹. The cobalt(II) complex is a d⁷ system. In octahedral field and at both low spin and high spin state, spin multiplicity in four. transition for ⁴t_{1g} → ⁴a_{2g} for low spin Co(II) aqua complex is expected at about 20,000 cm⁻¹ with a shoulder at about 16,000 cm⁻¹ for ⁴t_{1g}-⁴t_{1g}(p) and absorptivity below ≤ 20.00 dm³mol⁻¹. The results obtained are within the range expected for a low spin octahedral d⁷ [Co(PDP)₂]. Energies of 16867 and 13397 cm⁻¹ are due to of ligand effects.

HPDP coordinated as ONO donor. Possibility of charge transfer transition of ligand to metal or vice versa is not ruled out which will result in enhancement of ϵ_{\max} to about 40 dm³mol⁻¹cm⁻¹. [Cu(HPDP)₂Cl₂] is a d⁹ complex and is expected to suffer tetragonal distortion due to Jahn-Teller effects. One major absorption used is expected for this complex plus some splitting of band due to distortion arising from a symmetrical filling of orbit.

Therefore, the band at 428 nm with splitting shoulder below around 400 nm has been assigned to ²e_g → ²t_{2g} transition distort to a d_{4h} symmetry having the labels b_{1g} → a_{1g}, a_{1g} → b_{2g} and b_{2g} → e_g [23]. Only a_{1g} → b_{2g} and b_{2g} → e_g may be observed since b_{1g} → a_{1g} has very low energy as seen in the visible bearing a shoulder. This leads to a broadened band as seen in spectrum of [Cu(HPDP)₂Cl₂]. It is very much likely that [Cu(HPDP)₂Cl₂] is a distorted octahedral Cu(II) complex.

[Ni(PDP)₂] is a d⁸ complex with octahedral symmetry. It has two bands at 283 and 360 nm and absorptivity between 919 and 264 dm³ mol⁻¹cm⁻¹. Ni(II) complexes can assume various geometries [24] but in very strong field (for example CN⁻) square planar diamagnetic complexes are formed where less strong ligands from octahedral complexes. Bulky ligands can easily form tetrahedral complexes due to steric consideration. On the basis of stereochemistry and configuration, the bands at 283 nm with ϵ_{\max} of 919.11 dm³ mol⁻¹cm⁻¹ can be assayed to possible high energy charge transfer from ligand to metal ($\delta \rightarrow e_g$). Charge transfer to t_{2g} will be impossible because the Ni(II) t_{2g} level is filled. This will obscure any 3a_{2g}(f) → 3t_{1g}(p) transition. The band centered at 360 nm with molar absorptivity of 264.36 is assigned to 3a_{2g}(f) → 3t_{1g}(p) transition [23].

Infrared spectral data of HPDP and complexes

The special interest in the spectra are the functional groups involved in ligation of HPDP to the metal centers. The frequencies of functional groups in the free ligand was indicated by bands in the specific region. (3424-3211) cm⁻¹, (1820-1690) cm⁻¹ and (1670-1630) cm⁻¹, are consigned to the ν(N-H), ν(C=O) benzoyl and ν(C=O) pyrazolone, respectively.

The band at 3422(br) in HPDP shifted to lower frequency (3320, 3392, 3211) cm⁻¹ in the Fe(III), Ni(II), Co(II) complexes, respectively. This implies that the ligand coordinated to the metal centers via the -N-H group [25]. this broad band in the ligand remained almost same frequency (3424) cm⁻¹ in the Cu(II) complex, suggesting that it was free from bonding with the metal ion in the complex[26, 25].

The peak at 1820(w) in the ligand was assigned to ν(C=O) of benzoyl group. Similar observation has been reported by Suleman *et al.* [25, 27]. The shifting of these peaks to lower

frequencies in the complexes resulted the involving these bands in coordination with metal ions [28]. Also, the carbonyl group of the pyrazolone ring that absorbed at 1670 cm^{-1} shifted to lower frequencies in the complexes. This also suggests ligation from this group to the metal center [28]. The additional strong band appeared in the region $(1596)\text{ cm}^{-1}$ corresponding to the stretching vibrational of azomethin group $\nu(\text{C}=\text{N})$ of free ligand and are within same frequency ranges $(1597\text{--}1592)\text{ cm}^{-1}$ on their complexes, indicating non participation of $\text{C}=\text{N}$ group in coordination to metal ions [29]. The appearance of extra bands in the complexes spectra spanning the ranges of $(598\text{--}560)\text{ cm}^{-1}$, $(550\text{--}488)\text{ cm}^{-1}$ and 463 cm^{-1} can tentatively be linked to (M-O) [24], (M-N) [30] and (M-Cl) [26] interactions, respectively. This offers supplementary confirmation of the ligand's bonding with the metal ions [31].

No bands due to the enol (C-O) group was present and the broad bands at $3311\text{--}3422\text{ cm}^{-1}$ due to $\nu(\text{N-H})$ confirm formation of a hydrazone [32] and not an azo compound.

Nuclear magnetic resonance spectral data of HPDP and complexes

The $^1\text{H-NMR}$ spectrum of HPDP has chemical shift at 13.20 ppm which is assigned to H-N-proton of hydrozone that is more down field due to $\text{N-H}\cdots\text{O}$ intramolecular hydrogen bonding [23, 33]. The signal at 1.5971 ppm (2H, s) indicates trace water impurity whereas the methyl proton of the pyrazolone ring have chemical shifts 2.219 ppm (C- CH_3 ; 3H, s) and 3.0397 ppm (N- CH_3 ; 3H, s). The phenyl proton has the signals centered around $7.2841\text{--}7.660\text{ ppm}$ (10H, m) and $8.003\text{--}8.0314\text{ ppm}$ (5H, m) for β -diketone phenyls and 4-aminoantipyrine phenyl, respectively.

^1H NMR spectra of the complexes show multiplication of signals which are indecipherable. This is due to paramagnetic effects from the metal ions. This is also a confirmation of the formation of the complexes [16, 24, 26, 30].

$^{13}\text{C-NMR}$ spectrum of HPDP (Figure 2) shows 15 chemical shifts representing twenty-six carbons as shown in Figure 4. The signal at 194.02 represent the C1(acetyl carbon) where 191.11 ppm in for the C2 (pyrazolone) which are the most deshielded carbons. This is because these carbons are the most deshielded due to their proximity to electronegative atoms (such as oxygen and nitrogen) and the presence of multiple bonds (such as the carbonyl group). As a result, they experience a stronger effect from the magnetic field, leading to a higher chemical shift value. This indicate that the pyrazolone ring is the primary site of destruction, causing shifts in chemical shifts [34]. C3 and C4 have the signals at 144.44 and 144.95 ppm respectively whereas signals for C7 and C8 appears at 130.85 and 130.50 ppm , respectively.

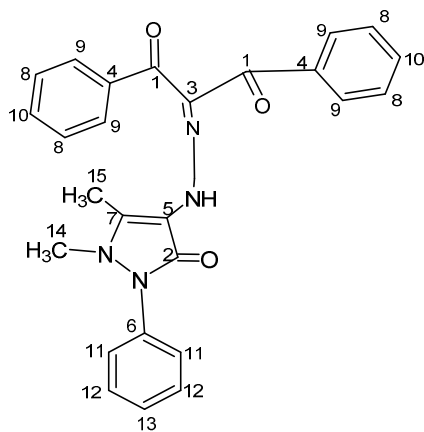


Figure 2. The structure of HPDP.

The other phenyl carbons of the C9, C10 and C11 have signals at 129.78, 129.58 and 121.58 ppm, methyl carbons, C14 and 15 chemical shift are situated at 34.37 and 31.77 ppm, respectively. C13 and C12 signals appear overlapping signal with C9 and C8 close to 130.00 ppm.

X-Ray crystallography data of HPDP

The X-ray crystallography properties of HPDP appear in Figure 3 and Table 4. HPDP crystallizes in monoclinic structure space group P2(1)/n or Pbc_a with unit cell dimensions $a = 9.5528(8) \text{ \AA}$, $\alpha = 90^\circ$; $b = 19.6260(16) \text{ \AA}$, $\beta = 101.421(6) \text{ \AA}$; $c = 12.058(10) \text{ \AA}$, $\gamma = 90^\circ$ for $z = 4$. X-ray diffractogram of HPDP recorded 24792 reflections for θ ranging between 2.02 to 28.01°. Selected bond length (Table 5) shows C(1)–O(1), C(13)–O(2) and C(15)–O(3) to be double bonds with lengths between 1.228–1.235 Å. Hydrogen bonding of O(3) to H(3) could have resulted slight lengthening of C(15)–O(3) bond. N(3)–N(4) and N(1)–N(2) are single bonds. N(3)–H(3A) confirms the hydrazone form of this compound with N(3)–N(4) single bond.

Table 4. Crystal data and structure refinement for HPDP.

Identification code	HPDP
Empirical formula	C ₂₆ H ₂₂ N ₄ O ₃
Formula weight	438.48
Temperature	372(2) K
Wavelength	0.71073 Å
Crystal system, space group	monoclinic, P2(1)/n
Unit cell dimensions	$a = 9.5525(8) \text{ \AA}$ $\alpha = 90 \text{ deg.}$ $b = 19.6260(16) \text{ \AA}$ $\beta = 101.421(6) \text{ deg.}$ $c = 12.0258(10) \text{ \AA}$ $\gamma = 90 \text{ deg.}$
Volume	2209.9(3) Å ³
Z, Calculated density	4, 1.318 mg/m ³
Absorption coefficient	0.088 mm ⁻¹
F(000)	F(000) 920
Crystal size	0.30 x 0.30 x 0.30 mm
Theta range for data collection	2.02 to 28.01 deg.
Limiting indices	-12 ≤ h ≤ 12, -25 ≤ k ≤ 21, -15 ≤ l ≤ 15
Reflections collected / unique	24792 / 5297 [R(int) = 0.1090]
Completeness to theta =	28.01 99.3 %
Max. and min. transmission	0.9740 and 0.9740
Refinement method	Full-matrix least-squares on F ²
Data / restraints / parameters	5297 / 0 / 301
Goodness-of-fit on F ²	0.967
Final R indices [I > 2σ(I)]	R1 = 0.0588, wR2 = 0.1369
R indices (all data)	R1 = 0.1166, wR2 = 0.1653
Extinction coefficient	0.0139(18)
Largest diff. peak and hole	0.363 and -0.337 e.Å ⁻³

Structures

The following conclusions were drawn based on the results of the qualitative chloride test, conductivity, infrared, UV-visible, NMR, microanalysis, mass spectroscopy, and XRD; HPDP exhibits the following characteristics: (i) monoclinic crystal structure; (ii) tridentate ligand with ONO ligation capabilities; (iii) cationic iron(III) complex; (iv) HPDP in a hydrazone with a =N-N-H moiety and an azo compound with a -N = N- group, respectively. The assigned structures to metal complexes are shown in Figure 4.

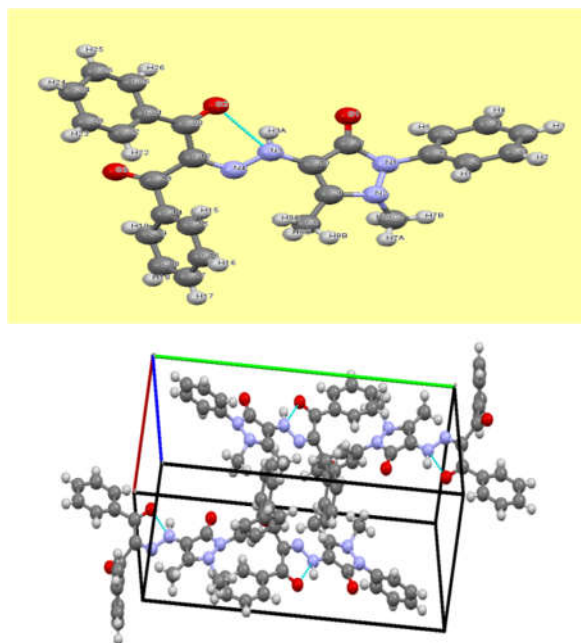


Figure 3. ORTEP diagram and crystal packing/hydrogen bonds of HPDP.

Antibacterial screening

The inhibition zone diameter (IZD) and minimum inhibitory concentration of the ligand and complexes are shown in Table 6. The results show HPDP to have activity against *Staphylococcus aureus*, *Proteus* and *Salmonella Typhi* but neutral to other microorganisms. Among the complexes, $[\text{Co}(\text{PDP})_2]$ shows activity only against *Streptococcus pneumoniae* while, $[\text{Ni}(\text{PDP})_2]$ is active against *Staphylococcus aureus* and *Salmonella typhi*. This means that $[\text{Co}(\text{PDP})_2]$ shows selective antibacterial activity against *Streptococcus pneumoniae*, making it a potential targeted therapeutic agent for treating pneumonia, meningitis, and other related infections. Its selectivity may reduce the risk of antibiotic resistance and minimize harm to beneficial microorganisms [35]. Also effectiveness of $[\text{Ni}(\text{PDP})_2]$ against *Staphylococcus aureus* (*S. aureus*) and *Salmonella typhi* (*S. typhi*), bacteria that cause skin infections, pneumonia, bloodstream infections, and typhoid fever shows its antibacterial activity against many pathogens, making it a potential therapeutic agent for treating related infections [19, 36]. The Microorganisms have no sensitivities to the Fe(III) and Cu(II) complexes. The trend of antibacterial activity could be due to the structure of the compounds and their degree of penetration to the cells of the microorganism [19]. Activity of HPDP against *Staphylococcus aureus* is better than the control drugs. Co(II) complex activity is a greater improvement compared to Gentamicin and Ciprofloxacin.

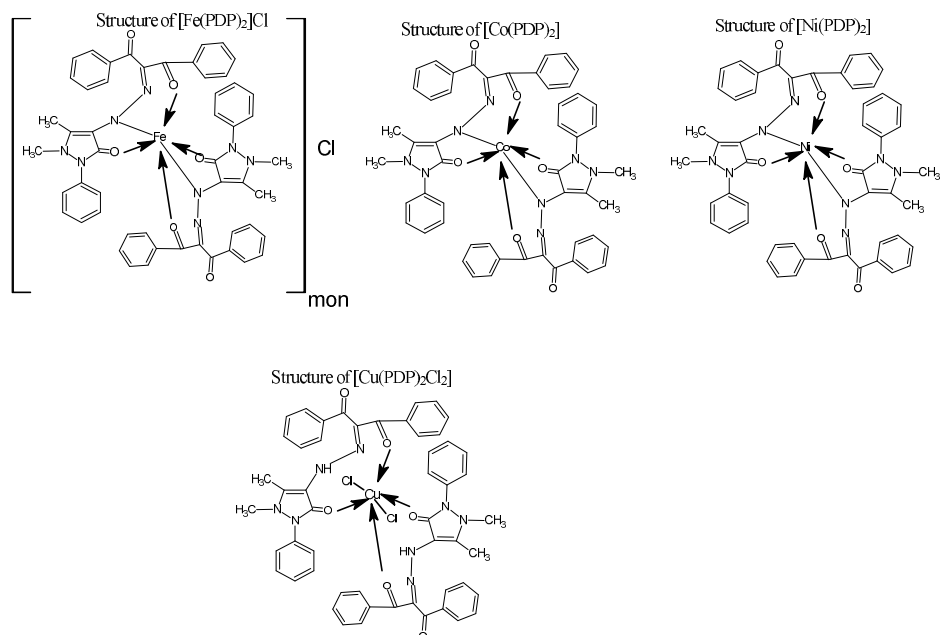


Figure 4. The structures of the metal complexes.

Table 5. Sensitivity test for HPDP and its complexes with some standard controls.

Microorganism	L ₁	L ₂	L ₃	L ₄	L ₅	A	G	C
<i>B. subtilis</i>	-	-	-	-	-	0.62	0.16	0.16
<i>S. pneumoniae</i>	-	25	-	-	-	100	2.5	2.5
<i>P. aeruginosa</i>	-	-	-	-	-	100	50	50
<i>E. coli (Eco 6)</i>	-	-	-	-	-	100	6.25	6.25
<i>E. coli (Eco 13)</i>	-	-	-	-	-	100	50	50
<i>S. aureus</i>	16	-	-	-	15	2.5	2.5	2.5
<i>Proteus mirabilis</i>	15	-	-	-	-	100	100	100
<i>S. intermedius (G101)</i>	-	-	-	-	-	2.5	2.5	2.5
<i>K. pneumoniae</i>	-	-	-	-	-	100	100	100
<i>S. typhi</i>	17	-	-	-	18			
Inhibition zone diameter (IZD) for HPDP and [Ni(PDP) ₂]								
Compound	Organism	Zone of inhibition (mm)						
		10 µg/cm ³	5 µg/cm ³	2.5 µg/cm ³	1.25 µg/cm ³	0.625 µg/cm ³	0.31 µg/cm ³	
L ₁	<i>S. typhi</i>	17	15	12	10	8	5	
	<i>S. aureus</i>	16	13	10	8	6	Nil	
	<i>P. mirabilis</i>	15	13	10	7	5	Nil	
L ₅	<i>S. aureus</i>	15	13	11	9	7	4	
	<i>S. typhi</i>	18	16	13	11	9	Nil	

Legend, L₁ = HPDP, L₂ = [Co(PDP)₂], L₃ = [Fe(PDP)₂]Cl, L₄ = [Cu(HPDP)₂Cl₂], L₅ = [Ni(PDP)₂], A = Ampicilin, G = Gentamicin and C = Ciprofloxacin.

CONCLUSION

The ligand HPDP and its Cu(II), Co(II), Ni(II), and Fe(III) complexes were successfully synthesised. Spectroscopic data and other assays revealed the following that HPDP crystallised as monoclinic crystals with a hydrozone formed by the PbCa space group. Due to its ligation characteristics, it coordinates via ONO groups in its structural motif, making it a terdentate ligand. The four metal complexes were paramagnetic and had Oh geometry. Neutral compounds with varying degrees of antibacterial activity are HPDP, [Co(PDP)₂], and [Cu(HPDP)₂Cl₂]. HPDP and [Ni(PDP)₂], were active on *Staphylococcus aureus* and *Salmonella typhi* up to the least concentration (0.31 µg/cm³) and therefore could be used as antibacterial drug.

REFERENCES

1. Ahmad, M.; Hameed, S.; Tahir, M.N.; Israr, M.; Anwar, M.; Shah, M.A.; Khan, S.A.; Din, G. Synthesis, characterization and biological evaluation of some 5-methylpyrazine carbohydrazide based hydrazones. *Pak. J. Pharm. Sci.* **2016**, *29*, 811-817.
2. Kölmel, D.K.; Kool, E.T. Oximes and hydrazones in bioconjugation: mechanism and catalysis. *Chem. Rev.* **2017**, *117*, 10358-10376.
3. Guo, R.; Chen J. Recent advances in the synthesis of fluorinated hydrazones. *RSC Adv.* **2018**, *8*, 17110-17120.
4. Verma, G.; Marella, A.; Shaquizzaman, M.; Akhtar, M.; Ali, M.R.; Alam, M.M. A review exploring biological activities of hydrazones. *J. Pharm. Bioallied Sci.* **2014**, *6*, 69-80.
5. Ali, A.; Khalid, M.; Rehman, M.A.; Anwar, F.; Zain-Ul-Aabidin, H.; Akhtar, M.N.; Khan, M.U.; Braga, A.A.; Assiri, M.A.; Imran, M. An experimental and computational exploration on the electronic, spectroscopic, and reactivity properties of novel halo-functionalized hydrazones. *ACS Omega* **2020**, *5*, 18907-18918.
6. Mohareb, R.M.; Ibrahim, R.A.; Moustafa, H.E. Hydrazide-hydrazones in the synthesis of 1,3,4-oxadiazine, 1,2,4-triazine and pyrazole derivatives with antitumor activities. *Org. Chem. J.* **2010**, *4*, 8-14.
7. Kumar, B.; Devi, J.; Dubey, A.; Tufail, A.; Antil, N. Biological and computational investigation of transition metal(II) complexes of 2-phenoxyaniline-based ligands. *Fut. Med. Chem.* **2023**, *15*, 1919-1942.
8. Jabeen, M. A comprehensive review on analytical applications of hydrazone derivatives. *Turk. Chem. Soc. Sect. A: Chem.* **2022**, *9*, 663-698.
9. Polović, S.; Ljolić, B.V.; Budimir, A.; Kontrec, D.; Galić, N.; Kosalec, I. Antimicrobial assesment of aroylhydrazone derivatives in vitro. *Acta Pharm.* **2019**, *69*, 277-285.
10. Ravesh, A.; Malhotra, R. Synthesis, characterization and antimicrobial screening of organotin(IV) complexes derived from Schiff bases of pyrazine-2-carboxylic acid hydrazone. *Asian J. Res. Chem.* **2018**, *11*, 262-268.
11. Kg, A. Metabolic syndrome-a new world-wide definition. A consensus statement from the International Diabetes Federation. *Diabet. Med.* **2006**, *23*, 469-480.
12. Zappitelli, M.; Ambalavanan, N.; Askenazi, D.J.; Moxey-Mims, M.M.; Kimmel, P.L.; Star, R.A.; Abitbol, C.L.; Brophy, P.D.; Hidalgo, G.; Hanna, M.; Morgan, C.M. Developing a neonatal acute kidney injury research definition: A report from the NIDDK neonatal AKI workshop. *Ped. Res.* **2017**, *82*, 569-573.
13. Deshmukh, P.; Soni, P.K.; Kankoriya, A.; Halve, A.K.; Dixit, R. 4-Aminoantipyrene: A significant tool for the synthesis of biologically active Schiff bases and metal complexes. *Int. J. Pharm. Sci. Rev. Res.* **2015**, *34*, 162-170.
14. Onufriev, A.V.; Alexov E. Protonation and pK changes in protein-ligand binding. *Q. Rev. Biophys.* **2013**, *46*, 181-209.

15. Yasuda, H. Infrared analysis of 2-pyrazolin-5-one derivatives. *Appl. spectrosc.* **1969**, 23, 22-28.
16. El-Saied, F.; Ayad, M.I.; Issa, R.M.; Aly, S.A. Synthesis and characterization of iron(III), cobalt(II), nickel(II) and copper(II) complexes of 4-formylazohydrazoneiline antipyrine. *Pol. J. Chem.* **2001**, 75, 773-783.
17. Balouri, M.; Sadiki, M.; Ibsouda, S.K. Methods for in vitro evaluating antimicrobial activity: A review. *J. Pharm. Anal.* **2016**, 6, 71-79.
18. Heatley, N.G. A method for the assay of penicillin. *Biochem. J.* **1944**, 38, 61-65.
19. Popiolek, Ł. Updated information on antimicrobial activity of hydrazide-hydrazones. *Int. J. Mol. Sci.* **2021**, 22, 9389-9408.
20. Yao, H.C.; Resnick, P. Azo-hydrazone conversion. I. The Japp-Klingemann reaction. *J. Am. Chem. Soc.* **1962**, 84, 3514-3517.
21. Mohanan, K.; Athira, C.J.; Sindhu, Y.; Sujamol, M.S. Synthesis, spectroscopic characterization and thermal studies of some lanthanide(III) nitrate complexes with a hydrazone derivative of 4-aminoantipyrine. *J. Rare Earths* **2009**, 27, 705-710.
22. Jeewoth, T.; Li Kam Wah, H.; Bhowon, M.G.; Ghoorohoo, D.; Babooram, K. Synthesis and anti-bacterial/catalytic properties of Schiff bases and Schiff base metal complexes derived from 2, 3-diaminopyridine. *Synth. React. Inorg. Matel-Org. Chem.* **2000**, 30, 1023-1038.
23. Hamidian, K.; Irandoust, M.; Rafiee, E.; Joshaghani, M. Synthesis, characterization, and tautomeric properties of some azo-azomethine compounds. *Zeitschrift für Naturforschung B.* **2012**, 67, 159-164.
24. Fouda, M.F.; Abd-Elzaher, M.M.; Shakhofa, M.M.; El-Saied, F.A.; Ayad, M.I.; El Tabl, A.S. Synthesis and characterization of a hydrazone ligand containing antipyrine and its transition metal complexes. *J. Coord. Chem.* **2008**, 61, 1983-1996.
25. Suleman, V.T.; Al-Daher, A.G. Synthesis, characterization, density functional theory studies and antioxidant activity of novel hydrazone ligands and their metal complexes. *Ori. J. Chem.* **2023**, 39, 1629-1642.
26. Pelli, M.; Del Gobbo, J.; Caviglia, M.; Gandin, V.; Marzano, C.; Karade, D.V.; Noonikara, P.A.; Dias, H.R.; Santini, C. Synthesis and investigations of the antitumor effects of first-row transition metal(II) complexes supported by two fluorinated and non-fluorinated β -diketonates. *Int. J. Mol. Sci.* **2024**, 25, 2038.
27. Abou-Melha, S.K.; Al-Hazmi, A.G.; Althagafi, I.; Alharbi, A.; Shaaban, F.; El-Metwaly, M.N.; El-Bindary, A. A. and El-Bindary, A. M. *J. Mol. Liq.* **2021**, 334, 116498
28. Gaber, A.; Belal, A. M. A.; El-deen, M. I.; Hassan, N.; Zakaria, R.; Alsanie, F.W.; Naglah, M. A. Refat, S.M. *Crystals* **2021**, 300, 1-17.
29. Mangalam, A.N.; Kurup, M.R.P.; Suresh, E.; Kaya, S.; Serdarovlu, G. *J. Mol. Struct.* **2021**, 1232, 129978.
30. Patel, A.K.; Jadeja, R.N.; Roy, H.; Patel, R.N.; Patel, S.K.; Butcher, R.J.; Cortijo, M.; Herrero, S. Copper(II) hydrazone complexes with different nuclearities and geometries: Synthesis, structural characterization, antioxidant SOD activity and antiproliferative properties. *Polyhedron* **2020**, 186, 114624.
31. Aly, S.A.; Hassan, S.S.; El-Boraey, H.A.; Eldourghamy, A.; Abdalla, E.M.; Alminderej, F.M.; Elganzory, H.H. Synthesis, biological activity, and the effect of ionization radiation on the spectral, XRD, and TGA analysis of Cu(I), Cu(II), Zn(II), and Cd(II) complexes. *Arabian J. Sci. Eng.* **2024**, 49, 361-379.
32. Sathyadevi, P.; Krishnamoorthy, P.; Jayanthi, E.; Butorac, R.R.; Cowley, A.H.; Dharmaraj, N. Studies on the effect of metal ions of hydrazone complexes on interaction with nucleic acids, bovine serum albumin and antioxidant properties. *Inorg. Chim. Acta* **2012**, 384, 83-96.
33. Hansen, P.E. A spectroscopic overview of intramolecular hydrogen bonds of NH...O,S,N type. *Molecules* **2021**, 26, 2409-2430.

34. Klepach, T.; Carmichael, I.; Serianni, A.S. ^{13}C -labeled N-acetyl-neuraminic acid in aqueous solution: Detection and quantification of acyclic keto, keto hydrate, and enol forms by ^{13}C NMR spectroscopy. *J. Am. Chem Soc.* **2008**, 130, 11892-11900.
35. Yahiaoui, R.Y.; den Heijer, C.D.; van Bijnen, E.M.; Paget, W.J.; Pringle, M.; Goossens, H.; Bruggeman, C.A.; Schellevis, F.G.; Stobberingh, E.E. APRES Study Team. Prevalence and antibiotic resistance of commensal *Streptococcus pneumoniae* in nine European countries. *Fut. Microbiol.* **2016**, 11, 737-744.
36. Schaffer, J.N.; Pearson, M.M. *Proteus mirabilis* and urinary tract infections. Urinary tract infections: *Mol. Path. Clin. Manag.* **2017**, 383-433.